OXFORD

Journal of AOAC INTERNATIONAL, 104(2), 2021, 355–367

doi: 10.1093/jaoacint/qsaa131
Advance Access Publication Date: 25 September 2020
Article

DRUG FORMULATIONS

Response Surface Methodology for Spectrophotometric Determination of Two β-Adrenergic Agonists-Terbium Chemosensors in Urine and Pharmaceutical Dosage Forms

Marwa Sakr,[1] Marwa Fouad ,[2,*] Rasha Hanafi ,[3] Hala Al-Easa[1], and Samir El-Moghazy[2]

[1]Department of Chemistry and Earth Sciences, College of Arts and Sciences, Qatar University, Doha 2713, Qatar, [2]Pharmaceutical Chemistry Department, Faculty of Pharmacy, Cairo University, Cairo 11562, Egypt, [3]Department of Pharmaceutical Chemistry, Faculty of Pharmacy and Biotechnology, German University in Cairo, Egypt

*Corresponding author's e-mail: Marwa.fouad@pharma.cu.edu.eg

Abstract

Background: According to literature reports, none of the previous methods of analysis had touched the multivariate approach for the quantification of significant factors affecting the interaction of dobutamine or hexoprenaline with Terbium.

Objective: Two novel β-adrenergic agonists-lanthanide chemosensors were prepared for the determination of dobutamine and hexoprenaline in their pure and pharmaceutical dosage forms and in urine samples. Fabrication of the two chemosensors was based on their ligand-metal interaction with the lanthanide Terbium.

Methods: A Plackett–Burman Design (PBD) was selected for the screening of four main variables (reaction time, metal volume, pH, and temperature). Applying Response Surface Methodology (RSM), a Central Composite Design (CCD) was executed for the optimization of the significant factors with narrower upper and lower limits. Spectrophotometric technique was exploited for the analysis of the two chemosensors.

Results: Maximum absorption was obtained at 299 and 298 nm for dobutamine-terbium and hexoprenaline-terbium complexes, respectively. Only factors that were found to bear significant effects on the formed complexes were promoted to the optimization level. Model verification was carried out, where target results coincided with those at the predicted levels, indicating the efficiency of the two proposed models. Validation of the proposed was implemented and linear ranges were found to be 3.30–13.50 and 1.90–10.00 μg/mL, for dobutamine and hexoprenaline, respectively.

Conclusions: Recovery and relative standard deviation values by application in pure powder, pharmaceutical dosage forms and spiked urine samples indicated high accuracy and reproducibility. Wide-ranging linear values and comparatively low detection limits inferred the effectiveness of the proposed method.

Highlights: RSM for optimization of spectrophotometric determination of dobutamine and hexoprenaline β-adrenergic agonists-lanthanide chemosensors; PBD was used for screening and CCD for optimization of variables affecting the

Received: 25 June 2020; **Revised:** 23 August 2020; **Accepted:** 10 September 2020

spectrophotometric method; Determination of dobutamine and hexoprenaline in pure powder, pharmaceutical dosage form, and spiked urine samples was accomplished after method validation.

β-Agonists are classified as synthetic phenyl ethanolamine compounds with the characteristic aromatic ring, β-hydroxyl group, and aliphatic nitrogen (1). Due to their high efficiency as bronchodilator and smooth muscle relaxant agents, their vital roles in human and veterinary medicine have also been reported (2).

Numerous techniques were previously described for the determination of β-agonists in biological fluids and in pharmaceutical formulations. These include high-performance liquid chromatography (3–5), gas and liquid chromatography with mass spectrometric detection (6–9), ultra-performance liquid chromatography tandem mass spectrometry (UPLC–MS/MS) (10), immunoassay (11–13), and electrochemical sensors (14,15).

Dobutamine hydrochloride (DOB-HCl), $C_{18}H_{23}NO_3$·HCl, 4–(2-((1-methyl-3–(4-hydroxybenzene) propyl) amido)ethyl)-1,2-dihydroxybenzene hydrochloric salt (Figure 1a) is a β_1 adrenergic receptor agonist with pronounced therapeutic effect for coronary heart failure and acute myocardial infarction (16). Several methods for the analysis of dobutamine (DOB) have been conveyed by literature, such as chemiluminescence (17), spectrofluorimetry (18), HPLC analysis employing spectrofluorimetric, electrochemical, UV detection (19–24), and other electrochemical techniques (25). Hexoprenaline sulphate (HEX-SO_4^{2-}), *N, N*-hexamethylene bis [2-amino-1–(3,4-dihydroxyphenyl)ethanol] sulphate (Figure 1b) is a selective β-sympathomimetic agent commonly used as a bronchospasmatic agent that can reduce bronchial exudation and enhance bronchial epithelium effectiveness. However, only a few methods for the determination of hexoprenaline were reported (26).

Due to the superior luminescent properties and extensive scope of applications of lanthanides in displays, sensors, biomarkers, researchers were prompted to further explore novel approaches for lanthanide determination and to observe their complexation nature with targeted ligands (27). Terbium complexes are commonly used in luminophores, lasers, and magnetic materials (28).

Multivariate regression and chemometric techniques are well thought-out as substitute techniques used for determination of authentic drugs in pharmaceuticals and biological fluids. Multivariate regression endorsed the analysis of various samples exhibiting diverse complexity with high accuracy and sensitivity. Recent literature reports clearly informed the superiority of applying chemometric-assisted analytical stratagem over conventional analytical techniques. For instance, the application of multiple response approach for the simultaneous determination of diclofenac, paracetamol, and ibuprofen in wastewater samples (29). Furthermore, multivariate-spectral analysis employed for the successful assay of different concentrations of phenylephrine HCl, doxylamine succinate, and paracetamol (in the presence of its impurity) in pharmaceutical dosage forms (30).

Multivariate analysis is also the favored method of assay for sample calibrations especially when interferences or spectra shifts are existent. It comprises a mathematically expressed regression equation along with comprehensive spectral statistical data useful for the selection of the optimum wavelength scheme that could be exploited for samples' calibration as well as for consequent chemometric model validations (31–34). Shedding the light on the diverse merits of utilizing Experimental Design (DoE) over traditional approaches, scientists benefited not only from conducting complex and numerous experiments at a faster rate, but also performing them at lower operating and development costs, hence maximizing progress and profit in analytical research and industrial applications, respectively. An interesting study of three β-lactam antibiotics (namely cefadroxil, cefprozil, and cefradine) was recently reported. The study assessed these drugs in industrial wastewater samples, applying chromatographic technique based on a two-level Factorial Design (FD) (32). In addition to its wide applications in the assay of pharmaceutical drugs, design of experiments was also exploited to determine vital hormones, such as estradiol valerate and norethisterone acetate-cyclodextrin complexes in their commercial formulations (33).

With an attempt to ensure that novelty of the proposed metal-ligand complexes was attained, the prime aim of this proposal was to focus on the novelty of the selected lanthanide metal as well as that of the drug selected for the complexation reaction. Literature survey revealed that, although terbium metal was extensively employed in a wide variety of industrial and pharmaceutical applications, yet no methods of analysis for neither DOB-Tb nor HEX-Tb complexes were reported.

In this study, a Plackett–Burman Design (PBD) efficiently pinpoints significant variables to a method relying on its aptitude to detect theoretically imperative variables with a fewer set of experiments. Accordingly, this screening design aimed to provide the optimal solution for conserving time and chemical consumption (34).

Among the most relevant multivariate techniques, Response Surface Methodology (RSM) showed substantial applications in analytical optimization. RSM is beneficial in determining the influence of operational factors for experimental development and optimization. One of the most frequent and competent methods exploited in RSM is Central Composite Design (CCD) (35). The current work reports on the development of a new, validated, fast, and sensitive spectrophotometric method by applying BPD for the screening of four main factors and CCD for the optimization of the significant factors. Therefore, it facilitates

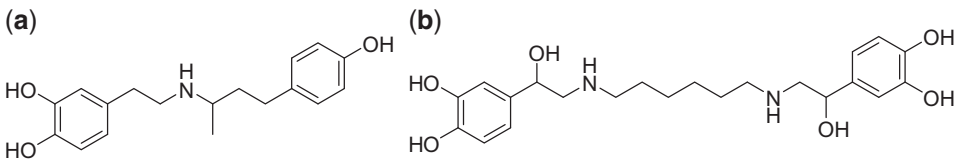

Figure 1. (a) Dobutamine and (b) hexoprenaline.

the quantitative determination of DOB and HEX in pure and pharmaceutical dosage forms as well as spiked urine samples.

Experimental

Materials and Reagents

All utilized reagents were of analytical grade. Doubly distilled water (DDW) was used throughout the work. Dobutamine and hexoprenaline were purchased from Sigma Aldrich (USA). Pharmaceutical formulations were purchased as follows: Dobier® 250 mg/5 mL ampoules (Chandra Bhagat pharma, Pvt. Ltd, India) and Gynipral® 0.50 mg tablets (Takeda Austria GmbH—NYCOMED GmbH - Austria).

Apparatus

An Agilent diode array UV-Vis spectrophotometer with 10 mm quartz cell was used for spectrophotometric measurements. A Jenway pH meter equipped with a glass combination electrode (UK) was used for adjusting pH of working solutions. A thermostatically controlled water bath was used throughout the work. Software employed for screening and optimization of experimental variables was Minitab®17 (Minitab Inc., State College, PA, USA).

General Procedure:

Using DDW, DOB, and HEX were prepared as 1 mg/mL stock solutions. To obtain appropriate concentrations and further dilutions were made within the working range 33–135 μg/mL for DOB and 19–100 μg/mL for HEX. Stock solution of Tb^{3+} was prepared as 0.373 mg/mL.

To enhance the stability of the formed Tb complexes, variables were screened as follows: reaction time (RT) from 0–30 min, metal volume (MV) 0.10–1.50 mL and temperature (T) was examined between 25–100°C by heating the mixtures in a thermostatically controlled water bath and pH 3.00–7.00. Mixtures were then diluted by DDW to 10 mL after which absorbance was recorded at λ 299 nm and λ 298 for DOB-Tb and HEX-Tb, respectively, against blank solutions.

Optimized Procedure for Pure Powder

To aliquots of standard solutions of DOB and HEX ranging from 33–135 and 19–100 μg/mL, respectively, a volume of 0.50 mL of 0.157 mg/mL Tb solution was added and pH was adjusted to 6.70 and 6.60 for DOB and HEX, respectively, by using phosphate buffer. The mixtures were heated, then the test-tubes were allowed to stand for 20 min to ensure completion of the complexation reaction. Adequate DDW dilutions were made and mixtures were transferred to 10 mL volumetric flasks.

Optimized Procedure for Pharmaceuticals and Urine Samples

(a) *Procedure for Dobier® ampoules*.—The content of 25 Dobier® ampoules was mixed and transferred into a 100 mL measuring flask and diluted to scale with DDW. Appropriate dilutions of the sample solution were performed to obtain final dilutions in range of (33–135 μg/mL).

(b) *Procedure for Gynipral® 0.50 mg tablets*.—50 tablets were weighed and ground. A sample of powder equivalent to 50 mg HEX was accurately weighed, then was extracted twice with water and filtered. The residue was then washed with DDW. The filtrate was then collected in 10-mL volumetric flasks, completed to volume with DDW. Aliquots of the solution were then diluted in the working range (19–100 μg/mL).

(c) *Procedure for spiked urine*.—The following components of spiked urine samples were weighed then dissolved in distilled water in a 1 L volumetric flask and stored in the refrigerator (Table 1).

Table 1. Spiked urine composition

Component	Weight, g
Sodium chloride	6.16
Sodium dihydrogen phosphate	5.03
Trisodium citrate	0.94
Magnesium sulfate	0.94
Sodium sulphate	2.40
Potassium chloride	4.74
Calcium chloride	0.84
Ammonium chloride	2.43
Urea	18.01
Creatinine	7.48

Table 2. Screened variables in PBD showing upper and lower limits

	Level	
Screened variable	Low (−)	High (+)
Reaction time (RT), min	0	30
Metal volume (MV), mL	0.10	1.50
Temperature (T), °C	25	100
pH	3.00	7.00

Screening (PBD) and Optimization Designs (RSM)

Four main variables were thoroughly scrutinized by using PBD design that comprised 16 runs and four central points. Upper and lower levels were adjusted, as shown in Table 2. Maximum absorbance responses (Y1 and Y2) for DOB-Tb and HEX-Tb for the four main variables, RT, MV, T, and pH were recorded. The magnitude of each variable on the anticipated response was presented by Pareto charts for standardized effect. Detection of significant factors in the designated multivariate analysis was also verified using ANOVA testing. After successful screening of variables, RSM was followed where CCD was employed for the optimization of the significant variables to achieve the optimal conditions required for enhancement of the proposed models.

Results and Discussion

Spectral Characteristics

The proposed procedure for the two designated models was reliant on the complexation reaction between the drug moiety (ligand) and Tb^{3+} (metal), where the formed DOB-Tb and HEX-Tb complexes revealed maximum absorbance at 299 and 298 nm, respectively. Maximum absorbance of pure DOB and HEX spectra was attained at 246 and 244 nm, respectively (Figure 2).

Determination of Significant Variables

(a) *Plackett–Burman for screening of variables*.—PBD was applied for screening of the four variables affecting the selected

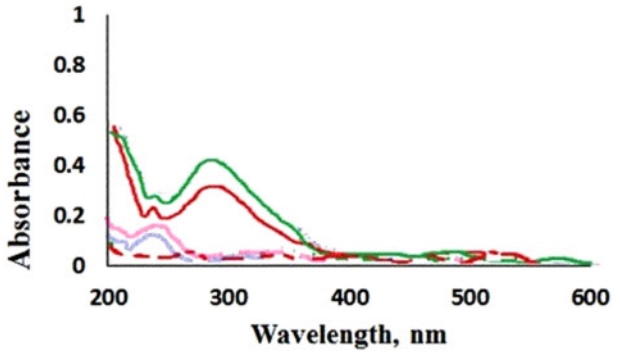

Figure 2. Absorption spectra of 10.00 μg/mL pure DOB (blue solid line) and HEX (purple solid line). Absorption spectra of 10.00 μg/mL DOB (red solid line) and HEX (green solid line) complexed with 0.50 mL of 0.157 mg/mL Tb against blank solution (red dotted line).

Table 3. PBD of experiments in coded levels for studying four variables

	Variables in coded units			
Run order	RT	MV	T	pH
1	1	−1	−1	−1
2	1	−1	1	−1
3	0	0	0	0
4	0	0	0	0
5	−1	−1	−1	−1
6	1	−1	1	1
7	−1	−1	−1	1
8	−1	1	1	1
9	−1	1	−1	−1
10	−1	−1	1	1
11	1	1	1	−1
12	1	1	−1	1
13	−1	1	1	−1
14	0	0	0	0
15	1	1	−1	1
16	0	0	0	0

responses, Y1 and Y2 (maximum absorbance for DOB-Tb and HEX-Tb, respectively), Table 3.

Three factors were found to be substantial for both Y1 and Y2 (Figure 3). While MV was the most influential factor in case of Y1 and Y2, RT was found to be the second important enhancer in case of Y1 followed by pH, unlike Y2 where the second weighty factor was pH, followed by RT. T showed no effect neither on Y1 nor Y2. The quality of fit in ANOVA and regression was obtained by means of residual plots (norm-plots and histograms) which proved that data followed normal distribution in case of Y1 and Y2, Figure 4. Additionally, ANOVA testing was implemented for the two designated models' validation, Table 4. Findings revealed the significance of only three main factors for both Y1 and Y2, which were found to be RT, MV, and pH, respectively, whereas T was proved insignificant suggesting that the spontaneity of the metal-ligand complexation reaction.

The obtained results were found to endorse the initial postulations where the obtained data clearly revealed that p-values were found to be <0.05 for the three significant

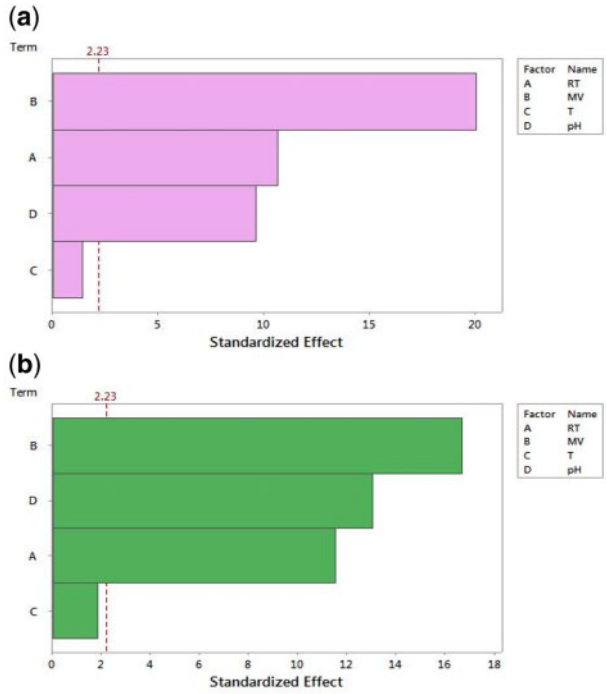

Figure 3. Pareto charts for standardized effects on applying PBD for (a) DOB and (b) HEX.

factors. Additionally, results with insignificant lack of fit (p-value >0.05) confirmed the triviality of experimental error for the two proposed models.

(b) *CCD for Optimization of screened variables.*—Subsequent to the screening phase, optimization of the three significant factors was attained by applying the RSM approach where a CCD, (36) was designated to compute the optimal conditions for R1 and R2.

In this phase, and only for the imperative factors, upper and lower limits of each variable were fine-tuned to include narrower ranges in comparison to the screening phase. In case of R1 and R2, the adjustment of ranges was as following, RT 10–20, MV 0.20–0.50, and pH 5.00–7.00. In order to follow a normal distribution pattern along with a constant variance, transformation of data was applied for R1 and R2, respectively. Hence, Box-Cox transformation at λ 0.5 (square root) was applied for R1 and R2, Figure 5. Following Box-Cox transformation, the transformed data indicated high p-values (>0.05) in normal probability plots and low Anderson-Darling (AD) values. AD is a statistical tool used to measure how well the data follow a particular distribution. For a specified data set and distribution, the better the distribution fits the data, the smaller this statistical value will be.

A second ANOVA test was performed to validate the outcomes of the optimization phase using CCD, Table 5. Backward elimination, one of the safest approaches, was applied for R1 and R2 in order to obtain reduced regression equations indicating only the significant variables.

After initial model construction, each term was first scrutinized by ANOVA, and variables were prudently removed from the model in a stepwise manner until the required significance was attained. The preeminence of the two models' ability to bear insignificant errors was once again indicated by the insignificance of the lack of fit. Moreover, R^2, R^2 adjusted, and R^2 predicted values derived from regression equations, confirmed the

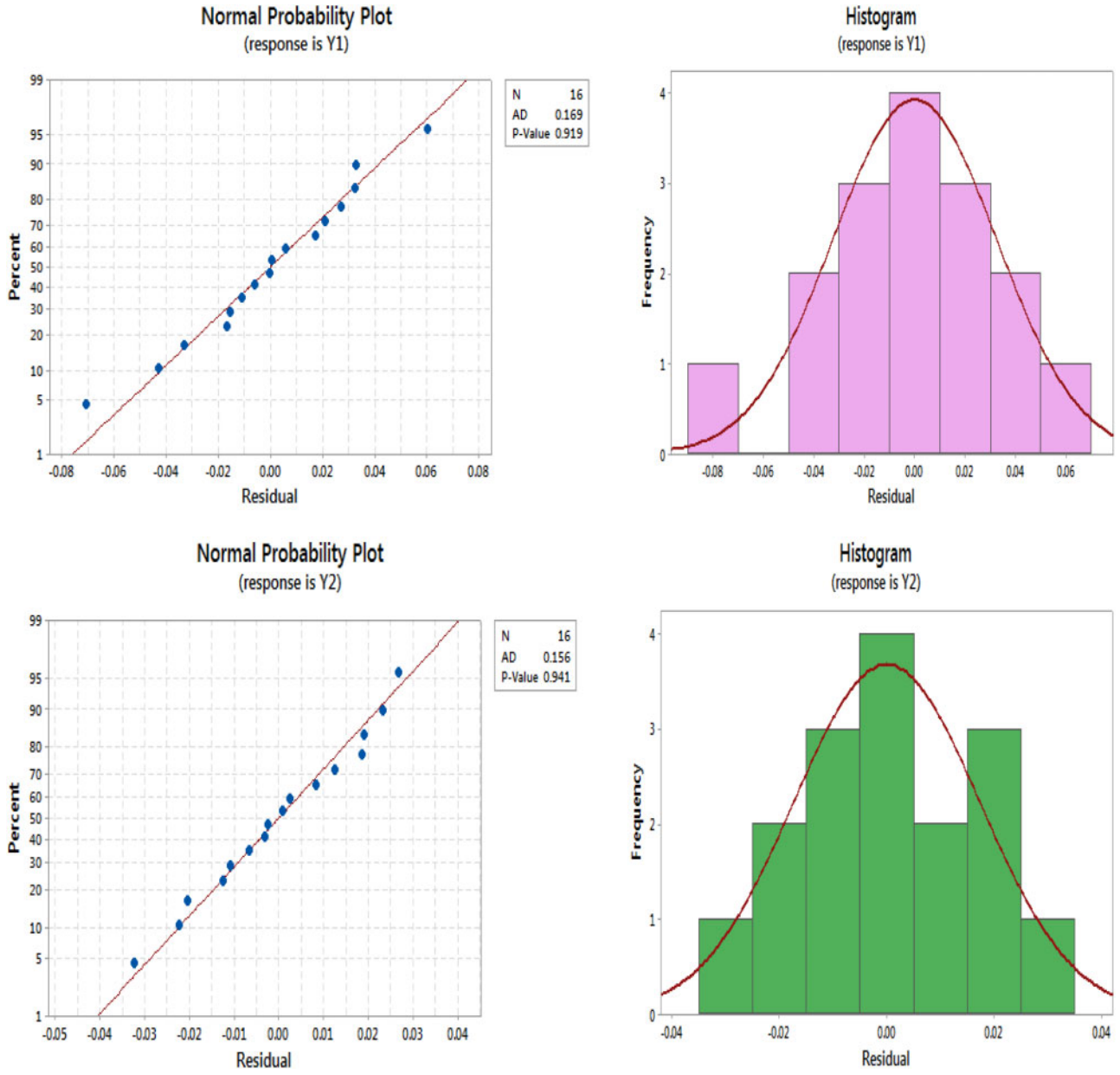

Figure 4. Residual plots for Y1 and Y2.

Table 4. ANOVA table for PBD for Y1 (A) and Y2 (B)

	A					B				
Source	DF	Adj SS	Adj MS	F-Value	P-Value	DF	Adj SS	Adj MS	F-Value	P-Value
Model	5	0.978112	0.195622	123.37	0.000	5	0.271777	0.054355	120.45	0.000
Linear	4	0.969201	0.242300	152.81	0.000	4	0.264647	0.066162	146.61	0.000
RT	1	0.181056	0.181056	114.19	0.000	1	0.060208	0.060208	133.42	0.000
MV	1	0.638485	0.638485	402.68	0.000	1	0.126075	0.126075	279.37	0.000
T	1	0.003136	0.003136	1.98	0.190	1	0.001564	0.001564	3.47	0.(0).092
pH	1	0.146523	0.146523	92.41	0.000	1	0.076800	0.076800	170.18	0.000
Curvature	1	0.008911	0.008911	5.62	0.039	1	0.007130	0.007130	15.80	0.003
Error	10	0.015856	0.001586			10	0.004513	0.000451		
Lack-of-Fit	6	0.012476	0.002079	2.46	0.201	6	0.003738	0.000623	3.22	0.139
Pure Error	4	0.003380	0.000845			4	0.000775	0.000194		
Total	15	0.993968				15	0.276290			

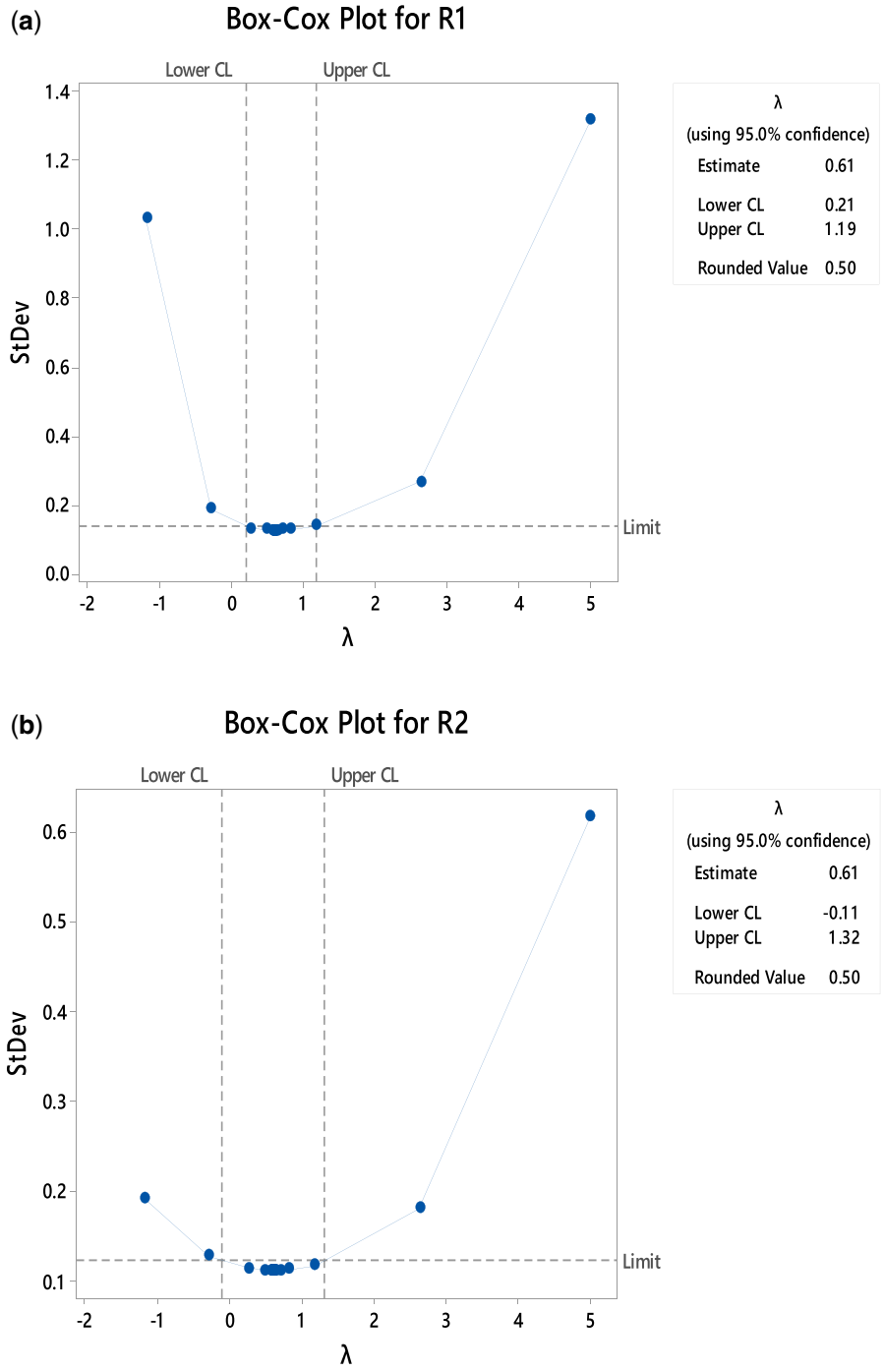

Figure 5. Box-Cox Plots for CCD for R1 (a) and R2 (b).

legitimacy of the optimized approaches for the proposed models after box-cox transformation, as demonstrated by Equations 1 and 2.

$$R1\,\hat{}\,0.5 = -1.476 + 0.02619RT + 0.140MV + 0.5897pH - 0.585MV * MV - 0.04915pH * pH - 0.003337RT * pH + 0.1380MV * pH \quad \text{(Eq. 1)}$$

where R^2, R^2 adjusted, and R predicted were 98.79, 98.09, and 96.00%, respectively.

$$R2\,\hat{}\,0.5 = -1.0796 - 0.000164RT + 0.5387MV + 0.4892pH - 0.8219MV * MV - 0.04315pH * pH + 0.01515RT * MV + 0.0775MV * pH \quad \text{(Eq. 2)}$$

where R^2, R^2 adjusted, and R^2 predicted were 99.59, 99.35, and 98.29%, respectively.

According to the regression Equations 1 and 2, it can be concluded that R1 and R2 exemplify direct proportionality with all linear effects, except for RT which shows an inverse relation in case of R2. On the other hand, all quadratic terms showed a

Table 5. ANOVA following Box-cox transformation and applying CCD for R1(A) and R2 (B)

	A					B				
Source	DF	Adj SS	Adj MS	F-Value	P-Value	DF	Adj SS	Adj MS	F-Value	P-Value
Model	7	0.553062	0.079009	140.32	0.000	7	0.405067	0.057867	414.14	0.000
Linear	3	0.332348	0.110783	196.75	0.000	3	0.242804	0.080935	579.23	0.000
RT	1	0.037029	0.037029	65.76	0.000	1	0.011559	0.011559	82.73	0.000
MV	1	0.163691	0.163691	290.72	0.000	1	0.187220	0.187220	1339.9	0.000
pH	1	0.131628	0.131628	233.77	0.000	1	0.044025	0.044025	315.08	0.000
Square	2	0.179173	0.089586	159.11	0.000	2	0.144365	0.072182	516.59	0.000
MV*MV	1	0.007923	0.007923	14.07	0.003	1	0.015627	0.015627	111.84	0.000
pH*pH	1	0.176797	0.176797	313.99	0.000	1	0.136287	0.136287	975.38	0.000
2-Way Interaction	2	0.024982	0.012491	22.18	0.000	2	0.008454	0.004227	30.25	0.000
RT*pH	1	0.011272	0.011272	20.02	0.001	1	0.004131	0.004131	29.56	0.000
MV*pH	1	0.013710	0.013710	24.35	0.001	1	0.004323	0.004323	30.94	0.000
Error	12	0.006757	0.000563			12	0.001677	0.000140		
Lack-of-Fit	7	0.005200	0.000743	2.39	0.178	7	0.001264	0.000181	2.18	0.203
Pure Error	5	0.001556	0.000311			5	0.000413	0.000083		
Total	19	0.559819				19	0.406744			

negative effect on both R1 and R2, unlike two-way interactions which explicated positive effects on both responses except for RT-pH in case of R2. RT-MV was excluded from Equation 1, while RT-pH was removed from Equation 2 for bearing non-significant effects. Overall, in order to obtain the simplest form for both equations, insignificant variable was cautiously removed by backward elimination.

Contour plots (2 D) and surface plots (3 D) were utilized to investigate the probable relationship between each pair of the three variables (37). X and Y variables are plotted on X and Y axis, respectively, and the response is represented by the contour lines, Figure 6. Furthermore, 3 D surface plot (Figure 7), provide a stronger idea of the paired variables' interactions.

The optimization plots (Figure 8) present the best-case scenario required to achieve the optimal conditions for the contributing variable blends (Table 6). The conditions illustrated by the graphs resulted in the maximum absorbance (target maximized) for R1 and R2. The individual desirability (d) for each single factor is expressed in the bottom section of the plot, with a value of 1 for of R1 and R2, respectively. Thus, it can be inferred that the target response has been successfully accomplished.

It is also worth mentioning that the optimal pH conditions for the proposed models based on the optimization plots results coincided with earlier literature reports, as in the past, studies revealed that lanthanide complexation reactions in aqueous medium were strongly associated with inclusion of a carboxylate- and phosphate-oxygen donors because of their oxophilicity. The role of the phenolic moiety as an anionic oxygen donor for lanthanide metal ions was only given minimal attention. This may be ascribed to the fact that the coordination of the phenolic lone pair is hindered by the weak acidity of the hydroxyl group, so since the lanthanide aqueous ions are themselves weak Lewis acids, they normally cannot compete with the hydrogen ion for complexation of phenol in water and precipitate as hydroxides in highly alkaline media.

Nevertheless, it has been informed that introduction of phenolic groups into an appropriately pre-structured configuration (catecholamine group) supremely enhanced the formation of strong and highly stable catecholamine-lanthanide (III) complexes.

Instead of employing a phenolate donor, Di Bernardo and others proposed that the introduction of a catechol moiety in tris(2,3-dihydroxybenzylamino) ethyl amine (TRENCAT) acting as binding units revealed high complexing aptitude toward lanthanide metal ions at approximately physiological pH (38,39).

Proposed Method Validation

The validation protocol for analytical method was based on, International Conference on Harmonization guidelines (ICH) (40). The proposed procedure for the determination of the two chemosensors in artificial urine was compared to the officially validated referenced methods. Recovery values were 99.75–100.35% and RSD 0.275% for DOB compared to 101.90–103.30% and RSD 2.80% of the cited method (41), while recovery values were 99.75–100.50 and 0.347% RSD for HEX compared to 97.50–102.40% and 0.65% to that of the referenced method (42).

Model Verification Tests

Three target points at the optimization stage were selected for the two models' verification. Table 7 reveals the confidence interval for response of these target points at 95%. The obtained findings were then compared to those at the predicted level. The experimentally obtained values were found to be reasonably close to those predicted and fell within the confidence intervals confirming the appropriateness and legitimacy of the proposed models.

LOD and LOQ

Calculated values of LOD and LOQ, were found to be 0.9641 and 2.9215 μg/mL for DOB, respectively, and 0.4815 and 1.4591 μg/mL for HEX, respectively. These low values inferred that the proposed technique is suitable for the determination of DOB and HEX in pure powder pharmaceutical dosage forms and spiked urine samples.

Accuracy and Precision

The accuracy and precision of the suggested method was determined for DOB and HEX; in pure powder, pharmaceutical dosage forms as well as spiked urine samples with three replicates for three different concentrations. Relative standard deviation values were computed, with values less than 1.

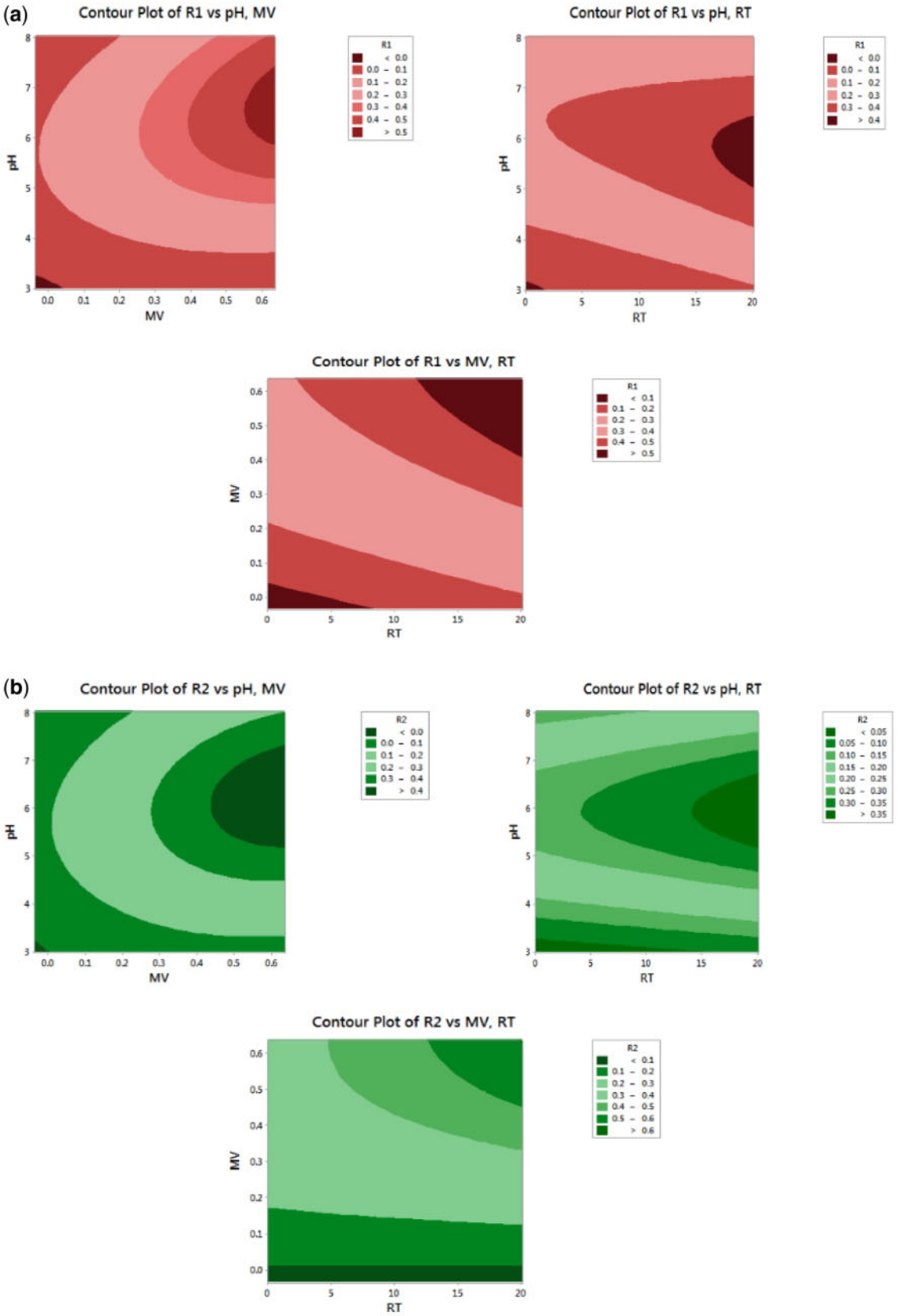

Figure 6. 2 D Contour plots for CCD showing R1 (a) and R2 (b) as a function of different variable paired interactions.

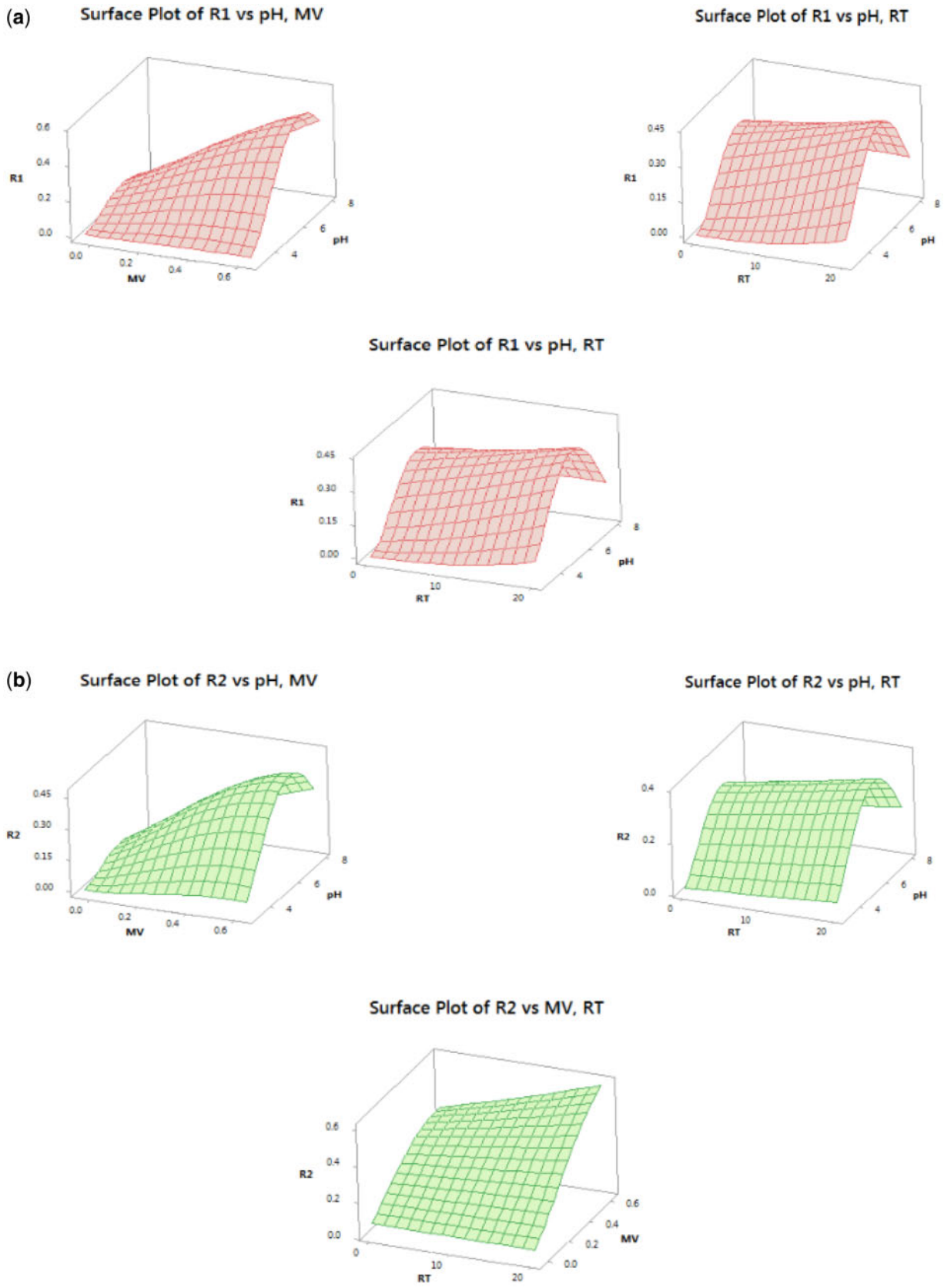

Figure 7. 3 D-Surface plots for CCD for revealing paired interactions of variables R1 (a) and R2 (b).

Figure 8. Desirability plots for R1 (a) and R2 (b).

Table 6. Optimal conditions for R1 and R2

	Optimized variables		
	RT, min	MV, mL	pH
DOB	20	0.50	6.70
HEX	20	0.50	6.60

Table 7. Verification tests for R1(DOB) and R2(HEX)

	Predicted levels RT	MV	pH	95% CI-low	Predicted	Absorbance 95% CI-high	Verification test results
R1							
Target-1	18	0.60	6.60	0.505176	0.571339	0.641572	0.586708
Target-2	21	0.55	6.90	0.480385	0.546146	0.616124	0.553945
Target-3	19	0.47	6.80	0.432888	0.470667	0.510026	0.471334
R2							
Target-1	19	0.55	6.90	0.464127	0.494152	0.525117	0.483914
Target-2	18	0.52	6.80	0.446209	0.468418	0.491167	0.472681
Target-3	21	0.47	6.70	0.458409	0.480904	0.503937	0.479990

Table 8. Determination of DOB (A) and HEX(B) in pure powder, pharmaceutical dosage form, and spiked urine samples using standard additions method

A								
Determination of DOB								
Pure powder			Dobier ampoule			Spiked urine		
Amt taken, μg/mL	Amt found, μg/mL	Recovery, %	Amt taken, μg/mL	Amt added, μg/mL	Recovery, %	Amt taken, μg/mL	Amt added, μg/mL	Recovery, %
3.3	3.295	99.840						
5	5.017	100.34	2.5	2.519	100.38	2.5	2.519	100.35
7	7.012	100.17	2.5	4.514	100.20	2.5	4.514	100.18
11	10.98	99.810	2.5	8.490	99.900	2.5	8.490	99.870
13.5	13.44	99.550	2.5	10.95	99.620	2.5	10.95	99.750
Mean		99.942			100.025			100.030
±SD		±0.313			±0.334			±0.276
RSD		0.313			0.334			0.275
B								
Determination of HEX								
Pure powder			Gynipral tablets			Spiked urine		
1.9	1.899	99.940						
4	4.012	100.300	1	3.017	100.420	1	3.017	100.500
6	5.997	99.950	1	4.995	99.910	1	4.995	99.800
8	7.995	99.930	1	6.999	99.980	1	6.999	99.750
10	9.977	99.770	1	8.987	99.870	1	8.987	99.900
Mean		99.978			100.045			99.987
±SD		±0.194			±0.254			±0.347
RSD		0.194			0.254			0.347

Table 9. Intra- and inter-day effects for the determination of DOB (A) and HEX (B) in pure powder, pharmaceutical dosage form, and spiked urine samples

(A)								
(a) Intra-day								
DOB in pure powder			DOB in Dobier ampoule			DOB in spiked urine		
Concn, μg/mL	Mean, % recovery ±SD	Error, %	Concn, μg/mL	Mean, % recovery ±SD	Error, %	Concn, μg/mL	Mean, % recovery ±SD	Error, %
3.3	100.325 ± 0.395	–0.325	3.3	99.285 ± 0.250	0.715	3.3	99.930 ± 0.535	0.070
7.0	99.635 ± 0.501	0.365	7.0	100.455 ± 0.507	−0.455	7.0	99.750 ± 0.389	0.250
13.5	99.8725 ± 0.810	0.127	13.5	99.740 ± 0.384	0.260	13.5	99.877 ± 0.559	0.122
(b) Inter-day								
.3.3	99.837 ± 0.490	0.162	.3.3	100.265 ± 0.247	–0.265	.3.3	100.112 ± 1.102	–0.112
7.0	100.180 ± 0.661	–0.180	7.0	100.557 ± 0.934	–0.557	7.0	99.955 ± 0.732	0.045
13.5	99.940 ± 0.617	0.060	13.5	99.950 ± 0.415	0.050	13.5	99.567 ± 0.766	0.432
(B)								
(a) Intra-day								
HEX in pure powder			HEX in Gynipral tablets			HEX in spiked urine		
1.9	100.055 ± 1.097	–0.055	1.9	100.202 ± 0.294	–0.202	1.9	99.950 ± 0.511	0.050
5.0	99.597 ± 0.317	0.402	5.0	99.252 ± 0.733	0.747	5.0	100.01 ± 1.137	–0.010
10	99.852 ± 0.608	0.147	10	99.770 ± 0.441	0.230	10	99.762 ± 0.614	0.250
(b) Intra-day								
1.9	99.570 ± 0.392	0.430	1.9	99.550 ± 0.552	0.450	1.9	99.937 ± 1.025	0.062
5.0	99.937 ± 0.747	0.062	5.0	99.877 ± 0.962	0.122	5.0	100.435 ± 0.568	–0.435
10	99.765 ± 0.210	0.235	10	99.412 ± 0.635	0.587	10	99.845 ± 0.692	0.155

Analytical Applications

The proposed procedure was used for the determination of the two β-adrenergic agonists in pure powder, pharmaceutical dosage forms, and spiked urine samples by implementing standard addition method where percentage recoveries were computed for DOB and HEX, Table 8.

In this work, artificial urine was used for preparing spiked samples. The analysis of biological fluids is essential for

monitoring the health of populations, but these measurements are difficult to implement in remote regions such as those found in less-industrialized countries, in emergency situations or in-home health-care settings

Urine is a variable fluid, both between individuals and in the same individual over time. It is more concentrated in the morning, and is affected by fluid intake, exercise, ambient temperature and diet. The pH can vary in the range 4.50–8.00 and the concentration of solute over a range of 4–5 times the average figures. For experimental purposes, urine can be collected from several individuals and pooled, but it will still vary significantly from batch to batch. Urine is produced in humans at about 1.00 mL/min, so in any experiment in which this rate is reproduced over an extended period, considerable quantities are required (43). That is why artificial urine is widely used in clinical trials instead of real urine to assure the consistency of the studied samples. Several studies revealed the merits of using artificial urine over real samples, for instance, in the determination of gemfibrozil (44), sparfloxacin (45), vital diuretics (46), and amino acids (47) in pharmaceutical and synthetic urine samples.

Robustness and Ruggedness

The influence of the small variation in the experimental parameters on the estimated response during the optimization steps was employed to evaluate robustness. Good desirability values were attained, pointing out the uniformity of the designated models during the repetitive application of the proposed procedure.

Reproducibility of the of the day to day obtained results was used as a fundamental measure that confirmed ruggedness. Inter- and intra-day variations were carried out and assessed for DOB and HEX, as demonstrated by Table 9.

Conclusions

PCD and Central Composite RSM were exploited to examine two β-adrenergic agonists-terbium complexes, namely DOB-Tb and HEX-Tb chemosensors. A multivariate approach was instigated to detect response affecting significant factors by the aid of PBD, after which optimization of the desired factors was carried out via CCD. The preliminary assumptions were further confirmed by quality tools measures, such as ANOVA testing, 2 D-contour, and 3 D-surface plots. Furthermore, determination of the two proposed β-adrenergic agonists, in pure powder, pharmaceutical dosage forms, and spiked urine samples indicated high accuracy and reproducibility. Wide-ranging linear values and comparatively low detection limits inferred the effectiveness of the proposed method.

Acknowledgments

We would like to thank Qatar University for the financial support provided by an internal grant.

Conflict of Interest

The authors declare that they have no conflict of interest

References

1. Slavíková, J., Kuncová, J., & Topolčan, O. (2007) *Clin. Cardiol.* **30**, 326–330. doi:10.1002/clc.20099
2. Giannetti, L., Ferretti, G., Gallo, V., Necci, F., Giorgi, A., Marini, F., Gennuso, E., & Neri, B. (2016) *J. Chromatogr. B Anal. Technol. Biomed. Life Sci.* **1036–1037**, 76–83. doi:10.1016/j.jchromb.2016.09.041
3. Asadian, E., Shahrokhian, S., Zad, A.I., & Jokar, E. (2014) *Sensors Actuators, B Chem.* **196**, 582–588. doi:10.1016/j.snb.2014.02.049
4. Blomgren, A., Berggren, C., Holmberg, A., Larsson, F., Sellergren, B., & Ensing, K. (2002) *J. Chromatogr. A* **975**, 157–164. doi:10.1016/S0021-9673(02)01359-6
5. Melwanki, M.B., Hsu, W.H., & Huang, S.D. (2005) *Anal. Chim. Acta* **552**, 67–75. doi:10.1016/j.aca.2005.07.036
6. Gallo, P., Brambilla, G., Neri, B., Fiori, M., Testa, C., & Serpe, L. (2007) *Anal. Chim. Acta* **587**, 67–74. doi:10.1016/j.aca.2007.01.034
7. Juan, C., Igualada, C., Moragues, F., León, N., & Mañes, J. (2010) *J. Chromatogr. A* **1217**, 6061–6068. doi:10.1016/j.chroma.2010.07.034
8. Domínguez-Romero, J.C., García-Reyes, J.F., Martínez-Romero, R., Martínez-Lara, E., Del Moral-Leal, M.L., & Molina-Díaz, A. (2013) *J. Chromatogr. B Anal. Technol. Biomed. Life Sci.* **923-924**, 128–135. doi:10.1016/j.jchromb.2013.02.008
9. Gressler, V., Franzen, A.R.L., de Lima, G.J.M.M., Tavernari, F.C., Dalla Costa, O.A., & Feddern, V. (2016) *J. Chromatogr. B Anal. Technol. Biomed. Life Sci.* **1015–1016**, 192–200. doi:10.1016/j.jchromb.2016.01.063
10. Zhang, Y., Liu, X., Li, X., Zhang, J., Cao, Y., Su, M., Shi, Z., & Sun, H. (2016) *Food Control* **60**, 667–676. doi:10.1016/j.foodcont.2015.09.010
11. Scippo, M.L., Weerdt, C.V.D., Willemsen, P., François, J.M., Rentier-Delrue, F., Muller, M., Martial, J.A., & Maghuin-Rogister, G. (2002) *Anal. Chim. Acta* **473**, 135–141. doi:10.1016/S0003-2670(02)00770-5
12. Danyi, S., Degand, G., Duez, C., Granier, B., Maghuin-Rogister, G., & Scippo, M.L. (2007) *Anal. Chim. Acta* **589**, 159–165. doi:10.1016/j.aca.2007.02.057
13. Cheng, G., Li, F., Peng, D., Huang, L., Hao, H., Liu, Z., Wang, Y., & Yuan, Z. (2014) *Anal. Biochem.* **459**, 18–23. doi:10.1016/j.ab.2014.05.005
14. Lin, X., Ni, Y., & Kokot, S. (2013) *J. Hazard. Mater.* **260**, 508–517. doi:10.1016/j.jhazmat.2013.06.004
15. Zhu, Q., Cai, F., Zhang, J., Zhao, K., Deng, A., & Li, J. (2016) *Biosens. Bioelectron.* **86**, 899–906. doi:10.1016/j.bios.2016.07.091
16. Albóniga, O.E., Alonso, M.L., Blanco, M.E., González, O., Grisaleña, A., Campanero, M.A., & Alonso, R.M. (2017) *J. Pharm. Biomed. Anal.* **145**, 178–185. doi:10.1016/j.jpba.2017.06.050
17. Liu, H., Zhang, L., Zhou, J., Hao, Y., He, P., & Fang, Y. (2005) *Anal. Chim. Acta* **541**, 123–127. doi:10.1016/j.aca.2004.11.071
18. Wei, S., Song, G., & Lin, J.M. (2005) *J. Chromatogr. A* **1098**, 166–171. doi:10.1016/j.chroma.2005.08.038
19. Alberts, G., Boomsma, F., Man in 't Veld, A.J., & Schalekamp, M.A.D.H. (1992) *J. Chromatogr. B Biomed. Sci. Appl.* **583**, 236–240. doi:10.1016/0378-4347(92)80558-8
20. Knoll, R., & Brandl, M. (1985) *J. Chromatogr. B Biomed. Sci. Appl.* **345**, 425–429. doi:10.1016/0378-4347(85)80183-3
21. Thippani, R., Pothuraju, N.R., Ramisetti, N.R., & Shaik, S. (2013) *J. Pharm. Anal.* **3**, 434–439. doi:10.1016/j.jpha.2013.07.003
22. Zimmermann, J., Dennhardt, R., & Gramm, H.J. (1991) *J. Chromatogr. B Biomed. Sci. Appl.* **567**, 240–247. doi:10.1016/0378-4347(91)80327-9
23. Yan, M., Webster, L.T., & Blumer, J.L. (2002) *J. Pharmacol. Exp. Ther.* **301**, 315–321. doi:10.1124/jpet.301.1.315

24. Patel, N., Taki, M., Tunstell, P., Forsey, P., & Forbes, B. (2012) *Eur. J. Hosp. Pharm.* **19**, 52–56. doi:10.1136/ejhpharm-2011-000027
25. Ghalkhani, M., & Salehi, M. (2017) *J. Mater. Sci.* **52**, 12390–12400. doi:10.1007/s10853-017-1361-6
26. Wedig, M., Thunhorst, M., Laug, S., Decker, M., Lehmann, J., & Holzgrabe, U. (2001) *J. Anal. Chem.* **371**, 212–217 doi: 10.1007/s002160100961
27. Matharu, K., Mittal, S.K., Ashok Kumar, S.K., & Sahoo, S.K. (2015) *Spectrochim. Acta Part A Mol. Biomol. Spectrosc.* **145**, 165–175. doi:10.1016/j.saa.2015.02.054
28. Vasylechko, V.O., Gryshchouk, G.V., Zakordonskiy, V.P., Vasylechko, L.O., Schmidt, M., Leshchack, I.M., Kalychak, Y.M., & Bagday, S.R. (2017) *Talanta* **174**, 486–492. doi: 10.1016/j.talanta.2017.06.052
29. Yehia, A.M., Elbalkiny, H.T., Riad, S.M., & Elsaharty, Y.S. (2020) *J. AOAC Int.* **103**, 257–264. doi:10.5740/jaoacint.19-0140
30. Yehia, A.M., Nabil, M., Badawey, A.M., & Abbas, S.S. (2020) *Spectrochim. Acta Part A Mol. Biomol. Spectrosc.* **239**, 118489.doi: 10.1016/j.saa.2020.118489
31. Monakhova, Y.B., Holzgrabe, U., & Diehl, B.W.K. (2018) *J. Pharm. Biomed. Anal.* **147**, 580–589. doi:10.1016/j.jpba.2017.05.034
32. Elbalkiny, H.T., Yehia, A.M., Riad, S.M., & Elsaharty, Y.S. (2019) *J. Anal. Sci. Technol.* **10**, 21.doi : 10.1186/s40543-019-0180-6
33. Arafa, R.M., Yehia, A.M., Abbas, S.S., & Amer, S.M. (2019) *Spectrochim. Acta Part A Mol. Biomol. Spectrosc.* **222**, 117237.doi: 10.1016/j.saa.2019.117237
34. Borges, P.R.S., Tavares, E.G., Guimarães, I.C., Rocha, R.D.P., Araujo, A.B.S., Nunes, E.E., & Vilas Boas, E.V.D.B. (2016) *Food Chem.* **210**, 189–199. doi:10.1016/j.foodchem.2016.04.077
35. Nemati, F., Zare-Dorabei, R., Hosseini, M., & Ganjali, M.R. (2018) *Sens. Actuat. B Chem.* **255**, 2078–2085. doi:10.1016/ j.snb.2017.09.009
36. El-Hamshary, M.S., Fouad, M.A., Hanafi, R.S., Al-Easa, H.S., & El-Moghazy, S.M. (2019) *Spectrochim. Acta Part A Mol. Biomol. Spectrosc.* **206**, 578–587. doi:10.1016/j.saa.2018.08.053
37. Sakr, M., Hanafi, R., Fouad, M., Al-Easa, H., & El-Moghazy, S. (2019) *Spectrochim. Acta Part A Mol. Biomol. Spectrosc.* **208**, 114–123. doi:10.1016/j.saa.2018.09.061
38. Sahoo, S.K., Baral, M., & Kanungo, B.K. (2006) *Polyhedron* **25**, 722–736. doi:10.1016/j.poly.2005.07.039
39. Liang, H., & Xie, F. (2009) *Spectrochim. Acta Part A Mol. Biomol. Spectrosc.* **73**, 309–312. doi:10.1016/j.saa.2009.02.031
40. ICH Topic Q2 (R1) Validation of Analytical Procedures: Text and Methodology (2005) in *International Conference on Harmonization*, http://www.ich.org/fileadmin/Public_Web_Site/ICH_Products/Guidelines/Quality/Q2_R1/Step4/Q2_R1__Guideline.pdf
41. Negahban, S., Fouladgar, M., & Amiri, G. (2017) *J. Taiwan Inst. Chem. Eng.* **78**, 51–55. doi:10.1016/j.jtice.2017.05.032
42. El-Nashar, R.M. (2008) *J. Autom. Methods Manag. Chem.* **2008**, 586310. doi:10.1155/2008/586310
43. Brooks, T., & Keevil, C.W. (1997) *Lett. Appl. Microbiol.* **24**, 203–206. doi:10.1046/j.1472-765X.1997.00378.x
44. Ardila, J.A., Oliveira, G.G., Medeiros, R.A., & Fatibello-Filho, O. (2013) *J. Electroanal. Chem.* **690**, 32–37. doi:10.1016/j.jelechem. 2012.11.038
45. Jan, M.R., Shah, J. ?0026; & Inayatullah, (2010) *J. Appl. Spectrosc.* **77**, 400–405. doi:10.1007/s10812-010-9345-1
46. Silva, E.F., Tanaka, A.A., Fernandes, R.N., Munoz, R.A.A., & da Silva, I.S. (2020) *Microchem. J.* **157**, 105027.doi: 10.1016/j. microc.2020.105027
47. Alevridis, A., Tsiasioti, A., Zacharis, C.K., & Tzanavaras, P.D. (2020) *Molecules* **25**, 1665. doi:10.3390/molecules 25071665